

Incidence-angle dependence of optical reflectivity difference from an ultrathin film on solid surface

J. P. Landry, J. Gray, M. K. O'Toole, and X. D. Zhu

Department of Physics, University of California, Davis, California 95616

Received October 3, 2005; accepted November 14, 2005; posted November 29, 2005 (Doc. ID 65123)

We studied the incidence-angle dependence of the optical reflectivity difference in response to ultrathin films on transparent and opaque substrates. We found that the classical three-layer model reproduces the experimentally obtained angular dependence for a monolayer of xenon on Nb(110) and for a monolayer of protein molecules on functionalized glass. We explore the enhancement of the optical response near the Brewster angle (or its equivalent for opaque substrates) in thin film detection. © 2006 Optical Society of America

OCIS codes: 240.0310, 310.6860, 170.5810.

Ellipsometry, in one form or another, measures changes in magnitude and phase of complex optical reflectivity (i.e., the Fresnel reflection coefficient) in response to changes on solid or liquid surfaces.¹ Examples of surface-bound changes are (1) the modification of morphology, as during erosion and homoepitaxy; (2) the addition and removal of ultrathin films, as during adsorption, desorption, heteroepitaxy, and other forms of growth; (3) reactions in a surface layer, including conformational changes of the layer and mass transports on and into the substrate. If one is not concerned with magnetic and chiral properties of the surface layer or the ultrathin film, relevant reflectivity changes are those for *p*-polarized (transverse magnetic) and *s*-polarized (transverse electric) components of an optical beam. At oblique incidence, in response to a surface-bound change, the magnitude and phase of the optical reflectivity change disproportionately for *p*- and *s*-polarized light. Optical ellipsometry measures such a disproportionate change.

A most sensitive form of ellipsometry is the oblique-incidence reflectivity difference (OI-RD) technique.² It is a polarization-modulated nulling ellipsometry that directly measures the difference in fractional reflectivity change between *p*- and *s*-polarized light. Let $r_{p0} = |r_{p0}| \exp(i\Phi_{p0})$ and $r_{s0} = |r_{s0}| \exp(i\Phi_{s0})$ be the respective reflectivity for *p*- and *s*-polarized light from a bare substrate surface, and let $r_p = |r_p| \exp(i\Phi_p)$ and $r_s = |r_s| \exp(i\Phi_s)$ be the respective reflectivity when an ultrathin film is deposited on the substrate or when the surface layer of the substrate is modified. The fractional reflectivity change is defined as $\Delta_p \equiv (r_p - r_{p0})/r_{p0}$ and $\Delta_s \equiv (r_s - r_{s0})/r_{s0}$. The difference in fractional reflectivity change is then $\Delta_p - \Delta_s$. When $\Delta_p - \Delta_s$ is small, $\text{Re}\{\Delta_p - \Delta_s\} \equiv (|r_p| - |r_{p0}|)/|r_{p0}| - (|r_s| - |r_{s0}|)/|r_{s0}|$ is simply the differential magnitude change; $\text{Im}\{\Delta_p - \Delta_s\} \equiv (\Phi_p - \Phi_{p0}) - (\Phi_s - \Phi_{s0})$ is the differential phase change. In terms of the ellipsometric ratio¹ $\rho \equiv r_p/r_s = \tan \psi \exp(i\delta)$, $\Delta_p - \Delta_s \equiv (\rho - \rho_0)/\rho_0$ with $\text{Re}\{\Delta_p - \Delta_s\} \equiv (\psi - \psi_0)/\sin \psi_0 \cos \psi_0$ and $\text{Im}\{\Delta_p - \Delta_s\} \equiv \delta - \delta_0$. The OI-RD technique has been successfully applied to the detection of a wide variety of ultrathin films and surface modifications ranging

from vapor-phase-deposited rare-gas films and perovskite oxide film in vacuum,²⁻⁶ to electrochemically deposited metallic films at liquid-solid interfaces,⁷ to microarrays of biological molecules on functionalized glass⁸ (i.e., gene chips and protein chips). To relate the structural and kinetic information on an ultrathin film or the modified surface layer on a substrate to the experimentally measured optical response and to reach the full potential of the OI-RD technique, one typically resorts to mean-field models of optics for multilayer films.⁹

Using a classical three-layer model to describe the optical response from the surface of a homogeneous substrate covered with an ultrathin film (or a modified surface layer), Zhu and co-workers^{10,11} have shown that

$$\Delta_p - \Delta_s \cong -i \left[\frac{4\pi\epsilon_s \tan^2 \theta \cos \theta}{\epsilon_0^{1/2}(\epsilon_s - \epsilon_0)(\epsilon_s/\epsilon_0 - \tan^2 \theta)} \right] \times \frac{(\epsilon_d - \epsilon_s)(\epsilon_d - \epsilon_0)}{\epsilon_d} \left(\frac{d}{\lambda} \right), \quad (1)$$

where θ is the incidence angle; ϵ_0 , ϵ_d , and ϵ_s are the optical dielectric constants of the ambient, the ultrathin film (or modified surface layer), and the substrate, respectively; d is the thickness of the film (or the modified surface layer). Changes at the surface other than thickness, such as mass density, chemical makeup, and morphology, are represented by the corresponding change in ϵ_d . For an ultrathin film with d and ϵ_d , $\Delta_p - \Delta_s$ also depends on θ . $\Delta_p - \Delta_s$ is maximized when the angular factor in Eq. (1) reaches the maximum. This occurs when the incidence angle is close to the Brewster angle θ_B on a transparent substrate or its equivalent on an opaque substrate.

In this paper we address two questions regarding the incidence-angle dependence of the optical reflectivity difference $\Delta_p - \Delta_s$. (1) Given that the three-layer model is a classical mean-field model, how well does Eq. (1) reproduce the angular dependence obtained from experiment? (2) To what extent can the sensitivity of $\Delta_p - \Delta_s$ to a surface-bound change be enhanced near the Brewster angle?¹² For the experiment, we

measure the optical reflectivity difference signals from two representative systems: (a) a monolayer of Xe on Nb(110) (a transparent film on an opaque substrate); (b) a monolayer of protein molecules on a functionalized glass substrate (a transparent film on a transparent substrate).

The optical arrangement and experimental procedures for obtaining $\Delta_p - \Delta_s$ have been described in detail by Thomas *et al.*² The Nb(110) sample is mounted on a manipulator inside an ultrahigh-vacuum chamber. With the manipulator and the available optical windows, we can vary the incidence angle θ from 25° to 85° within $\pm 1^\circ$. At each incidence angle θ , the clean Nb(110) substrate is held at 55 K and exposed to a Xe gas at 1.3×10^{-7} Torr. A saturated Xe double layer is formed under this steady-state condition.² When the Xe gas is evacuated from the chamber, the second monolayer of Xe desorbs and leaves behind a stable monolayer of Xe atoms. The optical reflectivity difference $\Delta_p - \Delta_s$ is measured during the Xe exposure and the subsequent desorption of the second monolayer, so that we have $\Delta_p - \Delta_s$ from one monolayer of xenon on Nb(110).

In Fig. 1 we display $\Delta_p - \Delta_s$ in response to adsorption of one monolayer of Xe on Nb(110) versus the incidence angle. To compare the measurements with the prediction of the classical three-layer model, we have computed $\Delta_p - \Delta_s$ by using Eq. (1). We use the following parameters in the calculation: $\lambda = 632.8$ nm for the probe He-Ne laser, $\epsilon_0 = 1$ for ambient (vacuum), $\epsilon_s = -0.25 + i16.13$ for the Nb substrate,¹³ $\epsilon_d = 2.19$ for the Xe monolayer,¹⁴ and $d = 0.355$ nm for the thickness of the Xe monolayer.¹⁵ The results are shown in Fig. 1 together with the experimental data. The calculated incidence-angle dependence agrees quantitatively with the experimental data. On an opaque substrate such as Nb(110), the equivalent of the Brewster angle (pseudo-Brewster angle) is the angle that maximizes the amplitude of $\cos \theta / (\epsilon_s \cot^2 \theta - 1)$ [another arrangement of

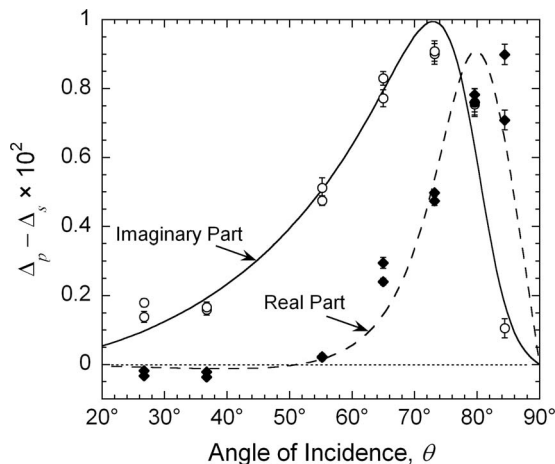


Fig. 1. $\Delta_p - \Delta_s$ in response to a monolayer of Xe on Nb(110) versus the incidence angle. Open circles, measured $\text{Im}\{\Delta_p - \Delta_s\}$; filled diamonds, measured $\text{Re}\{\Delta_p - \Delta_s\}$; solid curve, $\text{Im}\{\Delta_p - \Delta_s\}$ calculated by using Eq. (1) and the parameters listed in the text; dashed curve, $\text{Re}\{\Delta_p - \Delta_s\}$ calculated by using Eq. (1).

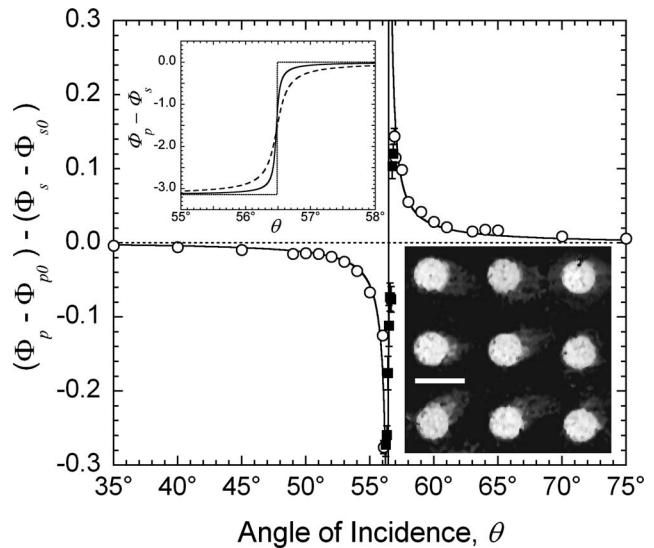


Fig. 2. $(\Phi_p - \Phi_{p0}) - (\Phi_s - \Phi_{s0})$ in response to a monolayer film of BSA molecules on glass versus the incidence angle (open circles and filled squares). The measured Brewster angle is $\theta_B = 56.48^\circ$. Top inset, $\Phi_p - \Phi_s$ versus the incidence angle calculated for a bare glass (dotted curve), an epoxide-derivatized glass (dashed curve), and an epoxide-derivatized glass covered with a monolayer of BSA molecules (solid curve). The difference between the solid curve and the dashed curve yields the solid curve in the main figure. Bottom inset, OI-RD image of the BSA spots obtained at $\theta = 55^\circ$. The scale bar is 200 μm .

the angular factor in Eq. (1)]. As shown in Fig. 2, both $\text{Im}\{\Delta_p - \Delta_s\}$ and $\text{Re}\{\Delta_p - \Delta_s\}$ peak near the pseudo-Brewster angle of $\theta_{PB} = 76.5^\circ$. We note that the peaks near the pseudo-Brewster angle are relatively broad, a point we will come back to below.

At the interface between two transparent materials, a true Brewster angle θ_B exists such that $\epsilon_s/\epsilon_0 = \tan^2 \theta_B$, and the peaks in $\Delta_p - \Delta_s$ near θ_B are much narrower in width and larger in amplitude. To compare the prediction of Eq. (1) with the experiment for an ultrathin film on a transparent substrate, we measure $\Delta_p - \Delta_s$ from a monolayer of bovine serum albumin (BSA, a protein) molecules on a functionalized glass slide. We use an oblique-incidence reflectivity difference scanning microscope as described previously by Landry and co-workers.⁸ With this microscope we can vary the incidence angle between 30° and 75° within $\pm 0.03^\circ$. The spatial resolution of the scanning microscope is 5 μm . BSA molecules in solution are printed as 150- μm spots on an epoxide-derivatized glass slide (CEL Associates) by using a contact-printing robot (Genetic Microsystems GMS 417). The BSA molecules in contact with the functionalized glass slide form a covalent bond with the slide.¹⁶ Excess BSA molecules and other unbound materials in the solution are washed off. After being spin dried in a centrifuge, the printed region (150 μm in diameter) of the glass slide is left with a monolayer of covalently bonded BSA molecules. The monolayer of BSA molecules on glass only yields $\text{Im}\{\Delta_p - \Delta_s\}$. This is expected from Eq. (1), since BSA molecules are also transparent at the He-Ne probe laser wavelength. At each incidence angle we obtain an image in

$\text{Im}\{\Delta_p - \Delta_s\}$ of the BSA-covered region on the slide, and from the image we deduce the averaged $\text{Im}\{\Delta_p - \Delta_s\}$ in response to a monolayer of BSA molecules on glass.

In Fig. 2 we display $\text{Im}\{\Delta_p - \Delta_s\}$ from a monolayer of BSA molecules on functionalized glass versus the incidence angle θ . Since the approximation of $(\Phi_p - \Phi_{p0}) - (\Phi_s - \Phi_{s0}) = \text{Im}\{\Delta_p - \Delta_s\}$ by Eq. (1) is no longer valid near θ_B , we have performed the full calculation of $(\Phi_p - \Phi_{p0}) - (\Phi_s - \Phi_{s0})$ from the three-layer model by using $\varepsilon_s = 2.28$ for the glass slide, $\varepsilon_d = 2.48$ (Ref. 17), and $d \approx 0.50$ nm (Ref. 18) for the BSA monolayer. The result is shown as the solid curve in Fig. 2. It overlaps with Eq. (1) at angles away from the Brewster angle $\theta_B = \tan^{-1}(\sqrt{\varepsilon_s/\varepsilon_0}) = 56.48^\circ$ but departs significantly from Eq. (1) near θ_B . Again the mean-field model reproduces the experimental data both away from and near θ_B within the experimental uncertainty. We note that the measured $(\Phi_p - \Phi_{p0}) - (\Phi_s - \Phi_{s0})$ in response to one monolayer of BSA molecules on glass peaks to 0.3 rad in magnitude at $\theta = 56.0^\circ$ (0.5° from θ_B), a factor of 30 increase from the value obtained at incidence angles 10° away from θ_B . The peak value from the experiment is less than the calculation, owing to a finite spread of incidence angles for the focused illumination beam used in our OI-RD microscope. It smoothes out the sharp peaks on both sides of θ_B . We also observed that the signal-to-noise ratio deteriorates when the incidence angle becomes very close to θ_B (particularly for filled squares in Fig. 2), presumably because of an increased sensitivity to the fluctuation in the pointing angle of the probe laser beam.¹⁹

We now come back to the two questions that we raised above. Clearly the classical three-layer model reproduces very well the experimental incidence-angle dependence of optical reflectivity difference $\Delta_p - \Delta_s$ for two ultrathin film-substrate systems. It is also clear that the sensitivity of $\Delta_p - \Delta_s$ to an ultrathin film (or modified surface layer) on a substrate is dramatically enhanced by the angular factor in Eq. (1) near the Brewster angle or the pseudo-Brewster angle.¹² Such an enhancement can be exploited to suppress the noises contributed from other optical components in an OI-RD setup that do not change when the incidence angle with respect to the sample is changed. One does need to control the pointing angle fluctuation $\delta\theta$ of the probe laser. For transparent films on transparent substrates, the signal-to-noise ratio in the experimentally obtained $\Delta_p - \Delta_s$ is limited by $|\theta - \theta_B|/\delta\theta$. On opaque substrates such as

Nb(110), the peaks in $\Delta_p - \Delta_s$ at the pseudo-Brewster angle are broad. As a result the noise contribution due to the pointing angle change of a probe laser beam can be minimized when the incidence angle is exactly at the pseudo-Brewster angle.

In conclusion, we have confirmed that the three-layer mean-field model adequately describes the incidence-angle dependence of $\Delta_p - \Delta_s$ from an ultrathin film (or modified surface layer) on a substrate. On an opaque substrate, $\Delta_p - \Delta_s$ is maximized at the pseudo-Brewster angle. On a transparent substrate, $\Delta_p - \Delta_s$ is maximally enhanced close to the Brewster angle θ_B .

This work is supported by the University of California under UC-GREAT grant 2004-09, and by a grant from the National Science Foundation Center for Biophotonics Science and Technology (CBST). X. D. Zhu's e-mail address is xdzhu@physics.ucdavis.edu.

References

1. R. M. A. Azzam and N. M. Bashara, *Ellipsometry and Polarized Light* (Elsevier Science, 1987).
2. P. Thomas, E. Nabighian, M. C. Bartelt, C. Y. Fong, and X. D. Zhu, *Appl. Phys. A* **79**, 131 (2004).
3. E. Nabighian, M. C. Bartelt, and X. D. Zhu, *Phys. Rev. B* **62**, 1619 (2000).
4. Y. Y. Fei, X. D. Zhu, L. F. Liu, H. B. Liu, Z. H. Chen, and G. Z. Yang, *Phys. Rev. B* **69**, 233405 (2004).
5. X. D. Zhu, W. Si, X. X. Xi, and Q. Jiang, *Appl. Phys. Lett.* **78**, 460 (2001).
6. F. Chen, T. Zhao, Y. Y. Fei, H. B. Lu, Z. H. Chen, G. Z. Yang, and X. D. Zhu, *Appl. Phys. Lett.* **80**, 2889 (2002).
7. W. Schwarzacher, J. Gray, and X. D. Zhu, *Electrochem. Solid-State Lett.* **6**, C73 (2003).
8. J. P. Landry, J. P. Gregg, and X. D. Zhu, *Opt. Lett.* **29**, 581 (2004).
9. J. D. E. McIntyre and D. E. Aspnes, *Surf. Sci.* **24**, 417 (1971).
10. A. Wong and X. D. Zhu, *Appl. Phys. A* **63**, 1 (1996).
11. X. D. Zhu, *Phys. Rev. B* **69**, 115407 (2004).
12. X. D. Zhu, "Comparison of two optical techniques for label-free detection of biomolecular microarrays on solids," *Opt. Commun.* (to be published).
13. J. H. Weaver, C. Krafska, D. W. Lynch, and E. E. Koch, *Phys. Daten* **18-1**, 127 (1981).
14. A. C. Sinnock, *J. Phys. C* **13**, 2375 (1980).
15. N. Stoner, M. A. van Hove, S. Y. Tong, and M. B. Webb, *Phys. Rev. Lett.* **40**, 243 (1978).
16. M. Schena, *Microarray Analysis* (Wiley, 2003), p. 50.
17. H. Arwin, *Appl. Spectrosc.* **40**, 313 (1986).
18. D. I. Svergun, M. V. Petoukhov, and M. H. J. Koch, *Biophys. J.* **80**, 2946 (2001).
19. J. Gray, P. Thomas, and X. D. Zhu, *Rev. Sci. Instrum.* **72**, 3715 (2001).